

MemShare: Memory Efficient Inference for Large Reasoning Models through KV Cache Reuse

Kaiwen Chen¹, Xin Tan¹, Minchen Yu², Hong Xu¹

¹The Chinese University of Hong Kong

²The Chinese University of Hong Kong, Shenzhen

Abstract

Large Reasoning Models (LRMs) have achieved significant advances in mathematical reasoning and formal logic tasks. However, their tendency to generate lengthy chain-of-thought sequences leads to substantial memory overhead during inference. We observe that LRMs frequently produce highly similar intermediate reasoning steps, which correspond to similar KV cache states across layers. Motivated by this observation, we propose MemShare, a novel KV cache management approach that effectively reduces memory overhead. MemShare employs a collaborative filtering algorithm to efficiently identify reusable KV cache blocks and enables zero copy cache reuse to significantly reduce memory overhead, improve throughput while maintaining accuracy. Experimental results demonstrate that MemShare delivers up to 84.79% improvement in throughput while maintaining better accuracy compared to existing KV cache management methods.

Introduction

The emergence of Large Reasoning Models (LRMs) such as OpenAI o1 (Jaech et al. 2024), QwQ-32B (Qwen 2025), and DeepSeek-R1 (Guo et al. 2025) has led to remarkable advances in solving mathematical and formal logic problems (Xu et al. 2025). LRMs engage in extended reasoning before producing a final answer. They generate lengthy chain-of-thought (CoT) sequences, explore multiple strategies, decompose problems into fine grained steps, and perform self verification.

However, the extended reasoning processes introduce significant memory overhead during inference. For instance, QwQ-32B can generate up to 13 redundant solutions for a simple question like “What is $2 + 3$?”, resulting in 1,953% more tokens than conventional models (Chen et al. 2024). When processing the AIME 24 (MAA 2025) dataset, it produces an average of 12,406 tokens per problem, requiring approximately 15GB of GPU memory per sequence for KV cache¹. Given that GPUs have memory capacities in the tens of GB, this substantial memory requirement severely limits the number of concurrent requests.

A key observation is that LRMs frequently generate similar reasoning steps, with highly similar contents recurring during solving problems, which we term *redundant thinking*.

¹Tested with Qwen team’s recommended sampling parameters: $Temperature = 0.6, TopP = 0.95, TopK = 20$

Question:

A curve is parameterized by $\{(x,y) = (t^3 + 7, -3t^2 - 6t - 5)\}$. Find the point the curve passes through at $t = 2$. Please reason step by step, and put your final answer within `\boxed{\{}}`.

Model’s Thoughts:

Okay, so I need to find the point that the curve passes through when t equals 2.

Starting with the x-coordinate: $x = t^3 + 7$.

2 cubed is 8. 8 plus 7 is 15.

Now for the y-coordinate: $y = -3t^2 - 6t - 5$.

Hmm, let me plug in $t = 2$ here step by step.

First, compute each term.

First term: $-3(4) = -12$

Second term: $-6*2 = -12$

Third term: -5

Adding the first two terms: $-12 - 12$ is -24 . Then adding -5 to that gives $-24 - 5 = -29$. Yes, that’s correct. So y is -29 at $t=2$.

Wait, let me verify that again because it’s easy to make a sign error here. Let me write it out step by step:

$y = -3(2)^2 - 6(2) - 5$

First term: $-3(4) = -12$

Second term: $-6*2 = -12$

Third term: -5

Adding the first two terms: $-12 - 12$ is -24 . Then adding -5 to that gives $-24 - 5 = -29$. Yeah, that’s right. So y is -29 at $t=2$.

The point (x, y) is $(15, -29)$.

Let me just make sure I didn’t mix up any numbers.

Wait, hold on, double-checking the x-coordinate again:

2 cubed is 8, plus 7 is 15.

So x is definitely 15.

I think that’s it. I don’t see any errors in my calculations.

Final Answer:

The point the curve passes through at $\{(t = 2)\}$ is `\boxed{\{(15, -29)\}}`.

Figure 1: An example of *redundant thinking* in reasoning models, as demonstrated by QwQ-32B.

Figure 1 provides a concrete example. More importantly, these similar steps exhibit highly similar KV cache states. Key and value vectors from similar reasoning steps remain closely aligned across transformer layers. This insight enables a clear optimization opportunity: by sharing similar KV cache blocks, we can significantly reduce memory overhead while preserving reasoning accuracy.

To exploit this insight, we propose MemShare, which employs a collaborative filtering algorithm that identifies reusable KV cache blocks through a two stage hierarchical process. First, it performs lightweight step-level comparisons using lexical similarity to narrow down candidate blocks, reducing computational overhead. Second, it precisely measures block-level Euclidean distances between key and value vectors to ensure reusability. This approach significantly mitigates memory overhead, increases throughput while maintaining accuracy.

Recent advances in KV cache management primarily exploit attention sparsity (Child et al. 2019; Zaheer et al. 2020; Ge et al. 2024) to reduce memory overhead. These methods can be categorized into three types: KV cache eviction, selective loading, and KV cache merging. Their core idea is to estimate the importance of tokens based on attention sparsity and then selectively discard, load, or merge tokens accordingly. However, these approaches have several limitations. First, attention sparsity varies significantly across transformer layers: shallow layers are typically denser, while deeper layers are sparser (Liu et al. 2024; Tang et al. 2024). Second, the set of critical tokens is highly query-dependent, making it challenging to generalize importance estimation (Tang et al. 2024; Tan et al. 2025). Consequently, these methods often rely on dynamic token-level or layer-level operations, which conflict with modern serving frameworks such as vLLM (Kwon et al. 2023) and SGLang (Zheng et al. 2024). Fine grained token or layer modifications disrupt block continuity, cause memory fragmentation and ultimately negate potential memory savings. In contrast, MemShare addresses these challenges by eschewing reliance on attention sparsity. Additionally, MemShare operates at the block-level, seamlessly aligning with vLLM and SGLang.

To validate the effectiveness of MemShare, we conduct comprehensive evaluations across a range of reasoning tasks. The results demonstrate that MemShare achieves substantial throughput gains: 84.79% for DeepSeek-R1-Distill-Qwen-32B on MATH-500 and 70.88% for QwQ-32B on MATH-500. MemShare outperforms existing KV cache management methods under comparable affected KV cache ratios. For example, on AIME 24 with Phi4-reasoning-plus (Abdin et al. 2025), MemShare achieves 0.766 accuracy, compared to Quest’s 0.6667 and SnapKV’s 0.336.

We make the following main contributions:

- We show that LRMs frequently generate highly similar intermediate reasoning steps (*redundant thinking*), suggesting that much of the KV cache content is similar.
- We introduce MemShare, a novel KV cache management method that efficiently identifies and reuses similar KV cache blocks.
- We comprehensively evaluate MemShare on a variety of reasoning tasks. The results show that MemShare achieves up to 84.79% throughput gains while maintaining model accuracy.

The rest of this paper is organized as follows: Background, Motivation, MemShare Details, Evaluation, Related Work, and Conclusion.

Background on LLM Inference

The Key Value (KV) cache is essential for efficient autoregressive inference in transformer based models, and the inference process consists of two distinct stages: prefill and decoding (Patel et al. 2024; Zhong et al. 2024).

Compute-Bound Prefill Stage During the prefill stage, the model processes the entire input sequence in parallel, performing computations such as matrix multiplica-

tions (GEMM) and attention calculations. The computational complexity of the attention mechanism scales quadratically with the sequence length, as it requires calculating interactions between all pairs of tokens (Shen et al. 2021).

The attention computation in the prefill stage can be formalized as follows. Let $X = (x_1, \dots, x_n) \in \mathbb{R}^{n \times d}$ denote the input sequence of hidden states, where n is the sequence length and d is the hidden state dimension. For each attention head h , the queries Q_h , keys K_h , and values V_h are computed as: $Q_h = XW_q^h, K_h = XW_k^h, V_h = XW_v^h$, where $W_q^h, W_k^h, W_v^h \in \mathbb{R}^{d \times d_h}$ are the projection matrices for head h , and d_h is the dimension of each head. The attention weight

A_h are then calculated as: $A_h = \text{softmax}\left(\frac{Q_h(K_h)^\top}{\sqrt{d_h}}\right)$. Finally,

the output of the attention head O_h is obtained by multiplying the attention weights with the values: $O_h = A_h V_h$.

Memory-Bound Decoding Stage During the decoding stage, the computation of attention weights and output vectors involves matrix-vector operations with low arithmetic intensity while requiring access to the entire historical KV cache. This creates a fundamental imbalance between the small amount of computation per step and the large memory required to store all KV cache. The size of the KV cache scales with both sequence length and batch size. For a 32B-parameter Qwen model, the KV cache requirements are particularly substantial: each token consumes 1280 KB of memory². A single 10K token request thus requires 12.2GB of memory solely for KV cache storage.

Paged Attention Driven by the pioneering work of vLLM (Kwon et al. 2023) and SGLang (Zheng et al. 2024), PagedAttention has become the dominant technology for high performance LLM inference.

In PagedAttention, the KV cache is partitioned into fixed size blocks. This shifts the granularity of KV cache management from the entire sequence to individual blocks, significantly improving memory efficiency. Importantly, while blocks can be stored non-contiguously in memory, the order of tokens within each block remains fixed, preserving the sequential structure required for attention computation.

Motivation

The section highlights two observations and introduces a theorem showing that reusing similar KV cache blocks has minimal effect on model accuracy.

Observation 1: Redundant thinking frequently occurs in the reasoning process of LRMs. During the reasoning process of LRMs, we frequently observe the emergence of highly similar reasoning patterns, a phenomenon we refer to as *redundant thinking*. This phenomenon is prevalent in large reasoning models (LRMs), as evidenced by both qualitative and quantitative analyses. Figure 1 provides an empirical example. To quantitatively assess redundant thinking, we conduct experiments in which each model is tasked with solving all problems in each dataset. For each dataset, the experiment is repeated five times, and the final results are

²Calculated as 2 (key/value vectors) x 5120 (hidden dimensions) x 64 (number of layers) x 2 (size of FP16)

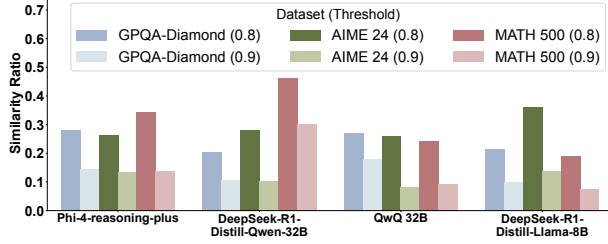


Figure 2: Redundant thinking across different reasoning models and datasets at varying similarity thresholds.

reported as the average across these runs to ensure statistical robustness. All experiments are performed using the officially recommended sampling parameters for each model. The reasoning model inherently segments the reasoning process into discrete steps, typically separated by delimiters like $\backslash n \backslash n$.

For each generated solution, we compute the cosine similarity between the tokenized embeddings of each reasoning step and all preceding steps (see Algorithm 1, Stage 1). We introduce the **similarity ratio** as a key metric, defined as the proportion of reasoning steps whose cosine similarity with any previous step exceeds a specified threshold. Here, the thresholds 0.8 and 0.9 correspond to high degrees of lexical similarity, with higher values reflecting stricter criteria.

The results can be seen in Figure 2. At a threshold of 0.8, 20-40% of the content is identified as redundant; at 0.9, this proportion decreases to 10-30%. Notably, *redundant thinking* is both model-agnostic and task-agnostic, appearing across models of different sizes and persisting across various datasets.

Observation 2: Redundant thinking leads to similar KV cache patterns in LRMs. Previous studies have explored token similarity within attention mechanisms. For example, D2O (Wan et al. 2025) employs cosine similarity between key states to identify merge candidates, while KVMerger (Wang et al. 2024) demonstrates token-level key state similarity within sequences. However, these studies do not examine the KV cache behavior in LRMs, which exhibit unique reasoning patterns, including *redundant thinking*.

To investigate whether *redundant thinking* correlates with KV cache similarity, we analyze block-wise Euclidean distance between KV caches. Our findings reveal a clear connection: as shown in Figure 3, heatmaps of key and value cache distances across layers 0 and 63 consistently show that lexically similar tokens exhibit smaller Euclidean distances (indicated by bluer regions). Among all block pairs, 8 out of 21 (approximately 38%) are identified as both lexically similar and possessing low Euclidean distance.

The above observations naturally motivate the idea of reusing KV cache blocks corresponding to similar reasoning steps to reduce memory overhead during inference. However, this approach raises a critical question: **Does reusing similar but not identical KV cache blocks adversely affect model accuracy?** To address this concern, we provide Theorem 1.

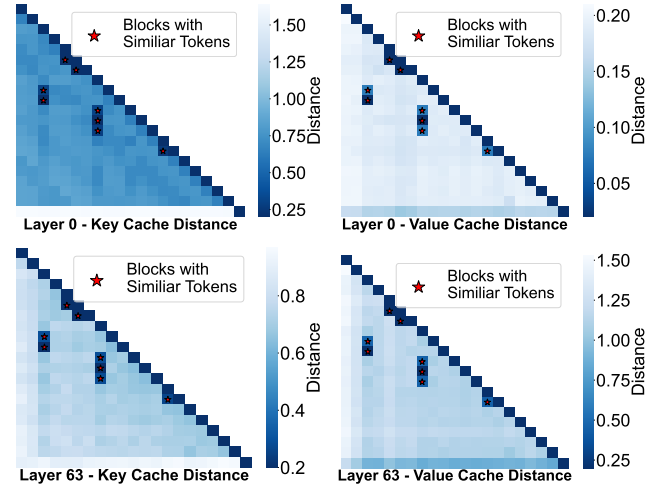


Figure 3: Block-wise Euclidean distance heatmaps for KV cache, generated using QwQ-32B on randomly sampled data from the MATH500 dataset.

Theorem 1. Let q_t be a query vector at step t , and let $K_t = [k_1, k_2, \dots, k_t]$ and $V_t = [v_1, v_2, \dots, v_t]$ denote the key and value caches, respectively. Suppose k_j is replaced by k'_j such that $\|k_j - k'_j\| < \epsilon$, and v_j is replaced by v'_j such that $\|v_j - v'_j\| < \delta$. Then:

1. The change in the attention score for position j satisfies

$$\|q_t k_j^\top - q_t k'_j{}^\top\| \leq \|q_t\| \cdot \|k_j - k'_j\| < \|q_t\| \epsilon.$$

The first inequality follows the Cauchy-Schwarz inequality. Consequently, the resulting attention weight $A^t = \text{softmax}\left(\frac{q_t K_t^\top}{\sqrt{d}}\right)$ is only minimally perturbed, as the softmax function is Lipschitz continuous (Virmaux and Scaman 2018; Collins et al. 2024).

2. The change in the output $o_t = \sum_{j=1}^t A_j^t v_j$ due to replacing v_j with v'_j is bounded by

$$\|A_j^t v_j - A_j^t v'_j\| = A_j^t \|v_j - v'_j\| < A_j^t \delta,$$

and the total perturbation in o_t is at most δ .

Therefore, substituting a key or value vector with a sufficiently close alternative induces only minor changes in the attention output, thereby justifying the validity of KV cache sharing. Rigorous proofs are provided in the Appendix, and empirical results are presented in the evaluation section.

MemShare

In this section, we introduce MemShare, a simple yet effective method designed to alleviate memory-bound constraints during decoding, thereby increasing batch size and throughput.

The design addresses two fundamental challenges: First, efficiently identifying reusable KV cache blocks requires careful consideration of granularity. Direct pairwise comparison of all KV cache blocks is computationally infeasible,

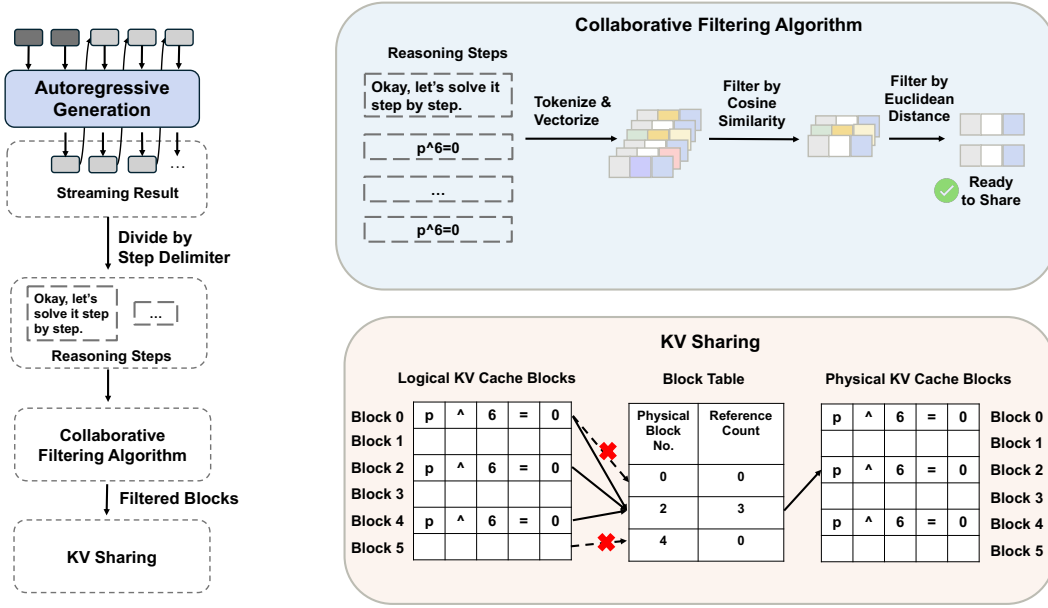


Figure 4: Main workflow of MemShare. The system consists of a Collaborative Filtering Algorithm and a Paged Attention Adapted KV Sharing Mechanism.

as it scales quadratically with sequence length ($O(n^2)$). Second, even after locating similar KV cache blocks, reusing them must not introduce GPU memory bandwidth overhead or disrupt the decoding process.

As illustrated in Figure 4, MemShare integrates two core components: a Collaborative Filtering Algorithm for efficient similarity search and a Paged Attention Adapted KV Sharing Mechanism for seamless reuse. Together, these components enable memory efficient decoding without compromising computational performance or accuracy.

Collaborative Filtering Algorithm LLMs exhibit *redundant thinking*, resulting in KV cache blocks with small Euclidean distance. To exploit this redundancy, Algorithm 1 employs a two stage similarity measurement process to efficiently identify reusable KV cache blocks. By combining step-level comparisons with block-level distance calculations, this approach achieves computational efficiency while preserving accuracy.

Stage 1: Step-Level Similarity Measurement This stage identifies lexically similar steps in the reasoning process by leveraging the model’s tokenizer to encode the textual content of each step. Each step is converted into a bag-of-words vector representation, and cosine similarity is computed between the current step s_{curr} and candidate steps s_{cand} .

We compare our tokenizer-based approach with alternative similarity measurement methods. Semantic embedding techniques like Sentence-BERT (Reimers and Gurevych 2019) capture contextual meaning, but they prove less suitable for identifying reusable reasoning steps compared to our lexical matching approach. Another implementation uses the model’s own embedding layers to encode steps,

while slightly more accurate, it introduces substantial computational overhead. Detailed comparison is shown in the evaluation part.

The tokenizer-based design delivers three key benefits: (1) It operates as a lightweight CPU-offloaded filter, avoid-

Algorithm 1: Collaborative Filtering Algorithm

Stage 1: Step-Level Similarity Measurement

Input: Current step s_{curr} , Candidate steps s_{cand} , Tokenizer \mathcal{T}

Output: Similarity scores sim_i

- 1: $\mathbf{v}_{curr} \leftarrow \mathcal{T}.\text{encode}(s_{curr})$
- 2: **for** each candidate step $s_i \in \{s_{cand}\}$ **do**
- 3: $\mathbf{v}_i \leftarrow \mathcal{T}.\text{encode}(s_i)$
- 4: $sim_i \leftarrow \frac{\langle \mathbf{v}_{curr}, \mathbf{v}_i \rangle}{\|\mathbf{v}_{curr}\|_2 \cdot \|\mathbf{v}_i\|_2}$
- 5: **end for**
- 6: **return** sim_i

Stage 2: Block-Level Distance Measurement

Input: KV cache blocks B_1, B_2 , KV cache Layers $\{\mathcal{L}_i\}_{i=1}^N$, Block size d , Number of KV heads h

Output: Normalized distance \bar{d}

- 1: $D \leftarrow 0$
 - 2: **for** each layer cache $(\mathbf{K}_i, \mathbf{V}_i) \in \{\mathcal{L}_i\}$ **do**
 - 3: $\Delta_K \leftarrow \|\mathbf{K}_i[B_1] - \mathbf{K}_i[B_2]\|_2$
 - 4: $\Delta_V \leftarrow \|\mathbf{V}_i[B_1] - \mathbf{V}_i[B_2]\|_2$
 - 5: $D \leftarrow D + (\Delta_K + \Delta_V) / (2dh)$
 - 6: **end for**
 - 7: **return** D/N
-

ing GPU computation during initial similarity screening; (2) The bag-of-words representation preserves exact lexical matches that frequently occur in redundant reasoning steps; (3) It reduces the calculation complexity from $O(n^2)$ to $O(K)$ (where $K \ll n$) by eliminating irrelevant comparisons early.

Stage 2: Block-Level Distance Measurement For steps flagged as similar in Stage 1, this stage computes the Euclidean distance between their corresponding KV cache blocks. The distance aggregates normalized differences between key-value vectors across all layers and attention heads. KV cache blocks with small Euclidean distance are flagged as reusable. Theorem 1 guarantees that such blocks yield bounded attention weight differences and output perturbations, ensuring accuracy.

While cosine similarity measures only angular alignment between vectors, Euclidean distance captures both directional and magnitude differences. This distinction is crucial for attention computation, where absolute values impact results. We also compared these two methods in the evaluation part. The results show that the euclidean distance achieves higher accuracy.

Paged Attention Adapted KV Sharing Mechanism Shown in Figure 4 and Figure 5, our KV sharing mechanism operates at the block-level, collaborating with VLLM’s block manager to enable zero-copy cache reuse. The evaluator identifies opportunities for KV cache sharing using Algorithm 1. Upon identifying shareable blocks, the mechanism simply updates the block table. During each decoding step, the scheduler manages the running, waiting, and swapped queues according to system resources, primarily memory availability. It batches requests that can be processed in parallel within the memory constraints, organizes the corresponding token IDs and block table information into the scheduler output, and forwards this to the model executor for inference.

This mechanism leverages VLLM’s decoupled CPU-GPU architecture by allowing the GPU model executor to immediately reuse shared blocks through simple updates to the CPU-managed block table, without interrupting the ongoing autoregressive generation process or consuming additional GPU memory bandwidth.

Evaluation

Settings We evaluate MemShare on the following benchmarks: AIME (MAA 2025), GPQA Diamond (Rein et al. 2023), and MATH-500 (Hendrycks et al. 2021). AIME assesses exceptional high school students in algebra, geometry, and number theory. GPQA Diamond comprises 198 graduate-level multiple choice questions in biology, physics, and chemistry. MATH-500 contains 500 high-school-level competition problems. By selecting these datasets, we ensure that our evaluation covers both mathematical and scientific reasoning, as well as varying levels of problem complexity. For our experiments, we select three reasoning models: DeepSeek-R1-Distill-Qwen-32B, QwQ-32B and Phi-4-reasoning-plus. We compare MemShare against a fully cached baseline and other methods, including

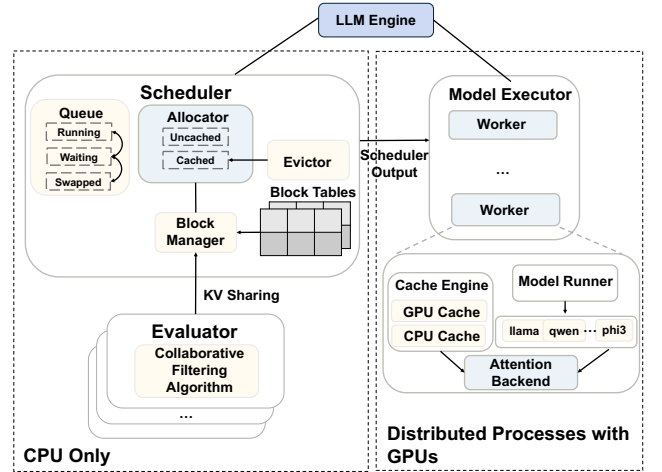


Figure 5: Paged Attention adapted KV sharing mechanism of MemShare.

StreamingLLM (Xiao et al. 2023), Quest (Tang et al. 2024) and SnapKV (Li et al. 2024).

MemShare employs a collaborative filtering algorithm to optimize KV cache sharing. At the step level, a similarity score is computed for each decoding step using Algorithm 1 (Stage 1). Steps with scores exceeding the predefined threshold (e.g., 0.8 or 0.9) proceed to the next stage. At the block level, Algorithm 1 (Stage 2) calculates pairwise distances between candidate blocks, selecting those with minimal distances for final sharing.

To simulate offline batch inference, all benchmark problems are submitted simultaneously. vLLM dynamically schedules requests based on system resources, particularly memory, adjusting batch size to maximize throughput. Experiments are performed on NVIDIA A800 GPUs (80GB) with Ubuntu 22.04.3 and vllm version 0.8.2. Each reported result is averaged over 5 independent runs.

Model	Threshold (Step, Block)	AIME 2024 Acc	AIME 2025 Acc	MATH 500 Acc	GPQA Diamond Acc
DeepSeek R1	0.8, 0.8	0.666	0.433	0.908	0.57
Distill	0.9, 0.8	0.677	0.4667	0.914	0.636
Qwen 32B	random	0.467	0.2	0.689	0.4074
	dense	0.733	0.533	0.927	0.631
QwQ-32B	0.8, 0.8	0.733	0.533	0.872	0.561
	0.9, 0.8	0.755	0.5667	0.894	0.591
	random	0.4	0.233	0.66	0.3888
	dense	0.766	0.633	0.894	0.611
Phi 4 reasoning plus	0.8, 0.8	0.7	0.6	0.883	0.469
	0.9, 0.8	0.766	0.633	0.895	0.505
	random	0.4334	0.133	0.642	0.3535
	dense	0.8	0.667	0.893	0.520

Table 1: Accuracy of MemShare across models and benchmarks using different threshold settings.

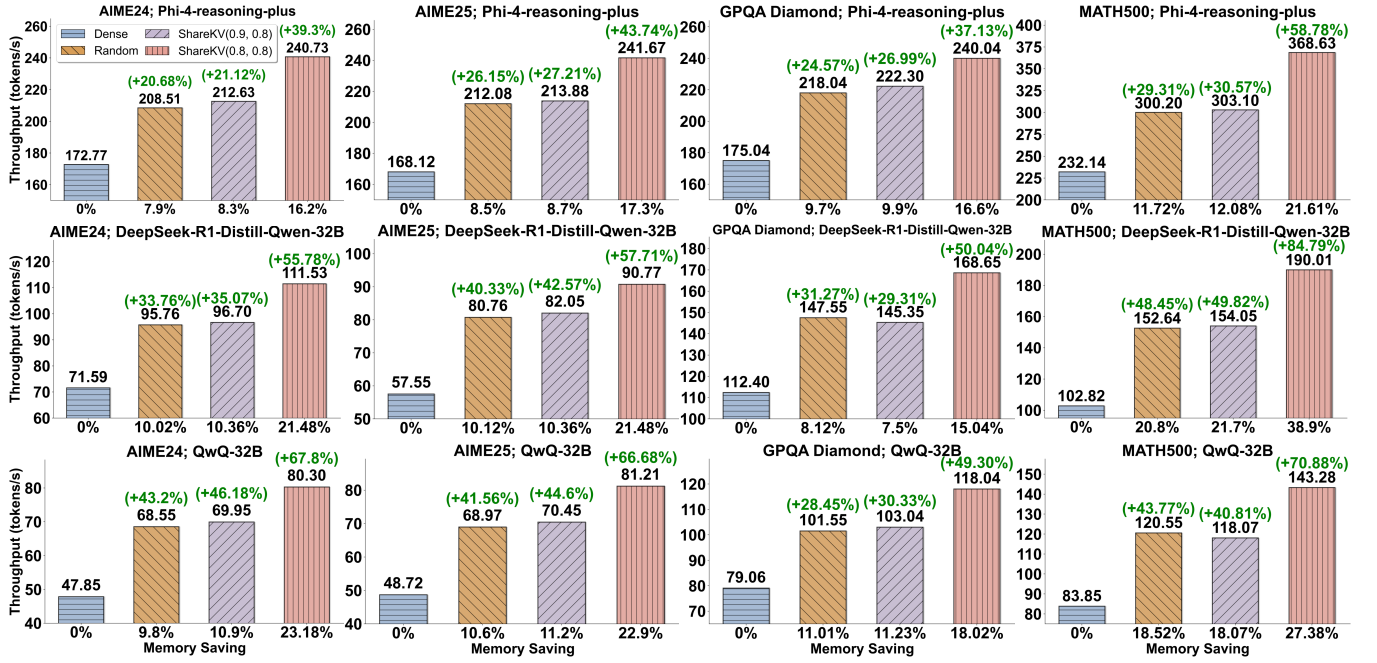


Figure 6: Performance of MemShare across models and benchmarks using different threshold settings.

Main Results We compare MemShare against two baseline settings: Dense Attention, which reserves all KV cache without sharing and Random Sharing, which reuses KV cache blocks arbitrarily. Table 1 and Figure 6 show the results. MemShare delivers significant throughput gains across all evaluated models and benchmarks. For example, on the MATH-500 benchmark, DeepSeek-R1-Distill-Qwen-32B achieves a 84.79% increase in throughput with a step similarity threshold of 0.8. Similar gains are observed in AIME 2024, where QwQ-32B achieves a 67.8% speedup. Despite these significant throughput gains, MemShare maintains model accuracy close to Dense Attention level. For example, on MATH-500, QwQ-32B retains 97.5% of its baseline accuracy (0.872 vs. 0.894) while achieving a 70.88% throughput boost.

Comparison with Other KV Cache Management Methods Table 2 presents a comprehensive comparison of various KV cache management methods across different models and benchmarks. The metrics include accuracy (Acc) and the affected ratio, where the affected ratio is defined as the proportion of tokens impacted by each KV cache management method relative to the total number of tokens. A higher affected ratio indicates a more aggressive policy, which may have a greater impact on model accuracy.

Under comparable affected ratios, MemShare consistently outperforms other methods in terms of accuracy. For example, in QwQ-32B, MemShare achieves 0.872 accuracy compared to Quest’s 0.506 on MATH-500. SnapKV, which is optimized for long prompts, demonstrates lower accuracy and is less effective in long decoding scenarios. StreamingLLM achieves moderate accuracy but suffers from information loss outside its sliding window.

Comparison with Different Similarity Measurement

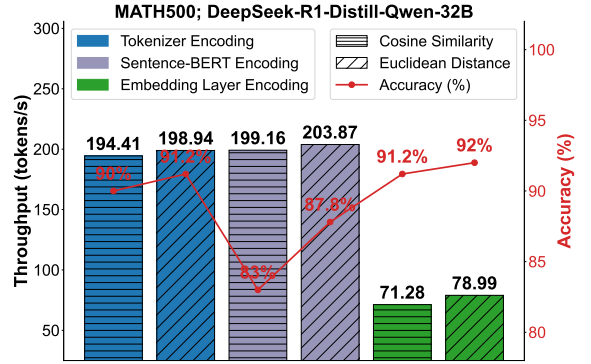


Figure 7: Performance comparison of similarity measurement algorithms. Algorithms are categorized in step-level (distinguished by colors) and block-level (distinguished by line patterns).

Methods We further evaluate the performance of different similarity measurement methods, as illustrated in Figure 7. Sentence-BERT is a lightweight Transformer-based model optimized for semantic similarity tasks. Specifically, we use all-MiniLM-L6-v2 in our experiments, which consists of 6 layers and 384-dimensional embeddings. This model efficiently encodes steps into dense vectors while preserving contextual meaning (e.g., recognizing mobile phone and smartphone as similar). We also assess the use of the model’s embedding layer for step encoding, which, while potentially more accurate, incurs higher computational costs due to increased dimensionality.

Tokenizer-based step encoding achieves higher accuracy

Model	Method	AIME 2024		AIME 2025		MATH 500		GPQA Diamond	
		Acc	Affected Ratio	Acc	Affected Ratio	Acc	Affected Ratio	Acc	Affected Ratio
DeepSeek R1 Distill Qwen 32B	StreamingLLM	0.5667	22.34%	0.333	20.7%	0.764	38.2%	0.4091	16.5%
	StreamingLLM	0.6	10.17%	0.366	12.1%	0.770	22.1%	0.4192	6.6%
	SnapKV	0.5	1.79% (66.7%)	0.2	1.8% (65.8%)	0.44	2.79% (48.7%)	0.2929	8.2% (81.2%)
	SnapKV	0.6	1.43% (55.6%)	0.233	1.47% (54.5%)	0.474	1.93% (31.62%)	0.3787	7.53% (74.9%)
	Quest	0.6	20.98%	0.333	25%	0.5	39.9%	0.5606	13.8%
	Quest	0.667	11.76%	0.467	13%	0.508	20.5%	0.606	7.6%
	MemShare	0.667	21.48%	0.433	20.9%	0.908	38.9%	0.5707	15.04%
	MemShare	0.677	10.36%	0.467	11.3%	0.914	21.7%	0.6364	7.05%
	Dense	0.733	0%	0.533	0%	0.927	0	0.631	0
QwQ 32B	StreamingLLM	0.5667	20.3%	0.367	20.6%	0.672	29.7%	0.5303	17.5%
	StreamingLLM	0.6	12.5%	0.4	11%	0.711	18.1%	0.5454	11.4%
	SnapKV	0.1	1% (67%)	0.233	1.43% (66.2%)	0.176	1.55% (50%)	0.1464	4.27% (81.3%)
	SnapKV	0.266	1.21% (56%)	0.233	1.13% (54.9%)	0.398	1.24% (32.66%)	0.2474	3.89% (75.1%)
	Quest	0.666	25.1%	0.533	23.5%	0.506	28%	0.5353	18.1%
	Quest	0.733	10.5%	0.533	9.1%	0.508	19.9%	0.5606	10.5%
	MemShare	0.733	23.18%	0.533	22.9%	0.872	27.38%	0.5606	18.02%
	MemShare	0.755	10.9%	0.567	11.2%	0.894	18.07%	0.5909	11.23%
	Dense	0.766	0%	0.633	0%	0.894	0	0.6111	0
Phi 4 reasoning plus	StreamingLLM	0.5667	16.6%	0.367	17%	0.522	23%	0.3333	18.9%
	StreamingLLM	0.6	10.6%	0.433	10%	0.546	13.7%	0.3434	9.6%
	SnapKV	0.2	2.56% (80.5%)	0.166	3% (80.3%)	0.146	4.76% (75.7%)	0.2525	7.29% (86.6%)
	SnapKV	0.366	1.96% (74.1%)	0.233	2.85% (73.8%)	0.226	4.38% (67.7%)	0.303	7% (82.17%)
	Quest	0.5667	18.5%	0.433	17.7%	0.518	21%	0.2121	17.8%
	Quest	0.6667	10.4%	0.433	9.9%	0.526	13.5%	0.2272	10.5%
	MemShare	0.7	16.2%	0.6	17.3%	0.883	21.61%	0.469	16.6%
	MemShare	0.766	8.3%	0.633	8.7%	0.895	12.08%	0.505	9.9%
	Dense	0.8	0%	0.677	0%	0.893	0	0.520	0

Table 2: Evaluation of different KV cache management strategies. For SnapKV, values in parentheses denote the ratio relative to total prompt KV cache.

than Sentence-BERT. For block similarity measurement, euclidean distance yields better accuracy. Although using the model’s embedding layer for encoding attains the highest accuracy, it incurs substantial computational overhead, resulting in approximately a 60% reduction in throughput.

Related Work

Recent work in KV cache management leverages the inherent sparsity of attention patterns to estimate the token importance. **Eviction-based methods** permanently discard tokens deemed less critical. Approaches such as H2O (Zhang et al. 2023) and SnapKV (Li et al. 2024) use importance scoring to evict tokens. StreamingLLM (Xiao et al. 2023) combines attention sinks with a fixed size cache. However, eviction is irreversible. Once evicted, KV cache cannot be recovered, even if later generation steps reveal their importance (Li et al. 2025). **Selective KV loading** methods, in contrast, retain the full KV cache but skip non-critical tokens during attention computation. Methods such as Quest (Tang et al. 2024) and SparQ (Ribar et al. 2023) exemplify this approach. These techniques reduce information loss but maintain the original memory footprint of the KV cache. **KV cache merging** methods combine less important tokens into more critical ones rather than discarding them entirely. Mini-

Cache (Liu et al. 2024) proposes an intra layer merging algorithm with restoration mechanisms to reduce memory usage. D2O (Wan et al. 2025) leverages cosine similarity between key states to select merge candidates and determine dynamic weights. However, the difficulty in accurately predicting which tokens are important for future text generation can lead to information loss, causing hallucinations (Yang et al. 2024; Bai et al. 2024).

Conclusion

We present MemShare, a novel KV cache management approach. MemShare efficiently identify and reuse similar KV cache blocks. Comprehensive evaluations demonstrate that MemShare achieves up to 84.79% throughput gains while maintaining accuracy. Compared to existing KV cache management methods under comparable affected cache ratios, MemShare consistently delivers better accuracy-efficiency trade-offs.

References

Abdin, M.; Agarwal, S.; Awadallah, A.; Balachandran, V.; Behl, H.; Chen, L.; de Rosa, G.; Gunasekar, S.; Javaheripi, M.; Joshi, N.; Kauffmann, P.; Lara, Y.; Mendes, C.

- C. T.; Mitra, A.; Nushi, B.; Papailiopoulos, D.; Saarikivi, O.; Shah, S.; Shrivastava, V.; Vineet, V.; Wu, Y.; Yousefi, S.; and Zheng, G. 2025. Phi-4-reasoning Technical Report. *arXiv:2504.21318*.
- Bai, G.; Liu, J.; Bu, X.; He, Y.; Liu, J.; Zhou, Z.; Lin, Z.; Su, W.; Ge, T.; Zheng, B.; et al. 2024. Mt-bench-101: A Fine-grained Benchmark for Evaluating Large Language Models in Multi-turn Dialogues. *arXiv preprint arXiv:2402.14762*.
- Chen, X.; Xu, J.; Liang, T.; He, Z.; Pang, J.; Yu, D.; Song, L.; Liu, Q.; Zhou, M.; Zhang, Z.; et al. 2024. Do Not Think That Much for $2+3=?$ on the Overthinking of o1-like LLMs. *arXiv preprint arXiv:2412.21187*.
- Child, R.; Gray, S.; Radford, A.; and Sutskever, I. 2019. Generating Long Sequences with Sparse Transformers. *arXiv preprint arXiv:1904.10509*.
- Collins, L.; Parulekar, A.; Mokhtari, A.; Sanghavi, S.; and Shakkottai, S. 2024. In-Context Learning with Transformers: Softmax Attention Adapts to Function Lipschitzness. In Globerson, A.; Mackey, L.; Belgrave, D.; Fan, A.; Paquet, U.; Tomczak, J.; and Zhang, C., eds., *Advances in Neural Information Processing Systems*, volume 37, 92638–92696. Curran Associates, Inc.
- Ge, S.; Zhang, Y.; Liu, L.; Zhang, M.; Han, J.; and Gao, J. 2024. Model Tells You What to Discard: Adaptive KV Cache Compression for LLMs. *arXiv:2310.01801*.
- Guo, D.; Yang, D.; Zhang, H.; Song, J.; Zhang, R.; Xu, R.; Zhu, Q.; Ma, S.; Wang, P.; Bi, X.; et al. 2025. Deepseek-r1: Incentivizing Reasoning Capability in LLMs via Reinforcement Learning. *arXiv preprint arXiv:2501.12948*.
- Hendrycks, D.; Burns, C.; Kadavath, S.; Arora, A.; Basart, S.; Tang, E.; Song, D.; and Steinhardt, J. 2021. Measuring Mathematical Problem Solving with the MATH Dataset. In *Proceedings of the Neural Information Processing Systems Track on Datasets and Benchmarks*, volume 1.
- Jaech, A.; Kalai, A.; Lerer, A.; Richardson, A.; El-Kishky, A.; Low, A.; Helyar, A.; Madry, A.; Beutel, A.; Carney, A.; et al. 2024. Openai o1 System Card. *arXiv preprint arXiv:2412.16720*.
- Kwon, W.; Li, Z.; Zhuang, S.; Sheng, Y.; Zheng, L.; Yu, C. H.; Gonzalez, J.; Zhang, H.; and Stoica, I. 2023. Efficient Memory Management for Large Language Model Serving with PagedAttention. In *Proceedings of the 29th Symposium on Operating Systems Principles*, 611–626.
- Li, Y.; Huang, Y.; Yang, B.; Venkitesh, B.; Locatelli, A.; Ye, H.; Cai, T.; Lewis, P.; and Chen, D. 2024. Snapkv: LLM Knows What You Are Looking for Before Generation. *Advances in Neural Information Processing Systems*, 37: 22947–22970.
- Li, Y.; Jiang, H.; Wu, Q.; Luo, X.; Ahn, S.; Zhang, C.; Abdi, A. H.; Li, D.; Gao, J.; Yang, Y.; and Qiu, L. 2025. SCBench: A KV Cache-Centric Analysis of Long-Context Methods. *arXiv:2412.10319*.
- Liu, A.; Liu, J.; Pan, Z.; He, Y.; Haffari, R.; and Zhuang, B. 2024. Minicache: KV Cache Compression in Depth Dimension for Large Language Models. *Advances in Neural Information Processing Systems*, 37: 139997–140031.
- MAA. 2025. American Invitational Mathematics Examination - AIME.
- Patel, P.; Choukse, E.; Zhang, C.; Shah, A.; Goiri, Í.; Maleki, S.; and Bianchini, R. 2024. Splitwise: Efficient Generative LLM Inference using Phase Splitting. In *2024 ACM/IEEE 51st Annual International Symposium on Computer Architecture (ISCA)*, 118–132. IEEE.
- Qwen. 2025. QwQ-32B: Embracing the Power of Reinforcement Learning.
- Reimers, N.; and Gurevych, I. 2019. Sentence-BERT: Sentence Embeddings Using Siamese BERT-Networks. In *Proceedings of the 2019 Conference on Empirical Methods in Natural Language Processing and the 9th International Joint Conference on Natural Language Processing (EMNLP-IJCNLP)*.
- Rein, D.; Hou, B. L.; Stickland, A. C.; Petty, J.; Pang, R. Y.; Dirani, J.; Michael, J.; and Bowman, S. R. 2023. GPQA: A Graduate Level Google-Proof QA Benchmark. *arXiv:2311.12022*.
- Ribar, L.; Chelombiev, I.; Hudlass-Galley, L.; Blake, C.; Luschi, C.; and Orr, D. 2023. Sparq Attention: Bandwidth-Efficient LLM Inference. *arXiv preprint arXiv:2312.04985*.
- Shen, Z.; Zhang, M.; Zhao, H.; Yi, S.; and Li, H. 2021. Efficient Attention: Attention with Linear Complexities. In *Proceedings of the IEEE/CVF winter conference on applications of computer vision*, 3531–3539.
- Tan, X.; Chen, Y.; Jiang, Y.; Chen, X.; Yan, K.; Duan, N.; Zhu, Y.; Jiang, D.; and Xu, H. 2025. DSV: Exploiting Dynamic Sparsity to Accelerate Large-Scale Video DiT Training. *arXiv:2502.07590*.
- Tang, J.; Zhao, Y.; Zhu, K.; Xiao, G.; Kasikci, B.; and Han, S. 2024. Quest: Query-Aware Sparsity for Efficient Long-Context LLM Inference. *arXiv:2406.10774*.
- Virmaux, A.; and Scaman, K. 2018. Lipschitz Regularity of Deep Neural Networks: Analysis and Efficient Estimation. *Advances in Neural Information Processing Systems*, 31.
- Wan, Z.; Wu, X.; Zhang, Y.; Xin, Y.; Tao, C.; Zhu, Z.; Wang, X.; Luo, S.; Xiong, J.; Wang, L.; et al. 2025. D2O: Dynamic Discriminative Operations for Efficient Long-Context Inference of Large Language Models. In *ICLR*.
- Wang, Z.; Jin, B.; Yu, Z.; and Zhang, M. 2024. Model Tells You Where to Merge: Adaptive KV Cache Merging for LLMs on Long-Context Tasks. *arXiv preprint arXiv:2407.08454*.
- Xiao, G.; Tian, Y.; Chen, B.; Han, S.; and Lewis, M. 2023. Efficient Streaming Language Models with Attention Sinks. *arXiv preprint arXiv:2309.17453*.
- Xu, F.; Hao, Q.; Zong, Z.; Wang, J.; Zhang, Y.; Wang, J.; Lan, X.; Gong, J.; Ouyang, T.; Meng, F.; et al. 2025. Towards Large Reasoning Models: A Survey of Reinforced Reasoning with Large Language Models. *arXiv preprint arXiv:2501.09686*.
- Yang, J. Y.; Kim, B.; Bae, J.; Kwon, B.; Park, G.; Yang, E.; Kwon, S. J.; and Lee, D. 2024. No Token Left Behind: Reliable KV Cache Compression via Importance-Aware Mixed Precision Quantization. *arXiv preprint arXiv:2402.18096*.

Zaheer, M.; Guruganesh, G.; Dubey, K. A.; Ainslie, J.; Al-berti, C.; Ontanon, S.; Pham, P.; Ravula, A.; Wang, Q.; Yang, L.; et al. 2020. Big Bird: Transformers for Longer Sequences. *Advances in neural information processing systems*, 33: 17283–17297.

Zhang, Z.; Sheng, Y.; Zhou, T.; Chen, T.; Zheng, L.; Cai, R.; Song, Z.; Tian, Y.; Ré, C.; Barrett, C.; et al. 2023. H2o: Heavy-hitter Oracle for Efficient Generative Inference of Large Language Models. *Advances in Neural Information Processing Systems*, 36: 34661–34710.

Zheng, L.; Yin, L.; Xie, Z.; Sun, C. L.; Huang, J.; Yu, C. H.; Cao, S.; Kozyrakis, C.; Stoica, I.; Gonzalez, J. E.; et al. 2024. Sglang: Efficient Execution of Structured Language Model Programs. *Advances in Neural Information Processing Systems*, 37: 62557–62583.

Zhong, Y.; Liu, S.; Chen, J.; Hu, J.; Zhu, Y.; Liu, X.; Jin, X.; and Zhang, H. 2024. DistServe: Disaggregating Prefill and Decoding for Goodput-Optimized Large Language Model Serving. In *18th USENIX Symposium on Operating Systems Design and Implementation (OSDI 24)*, 193–210.

Proof of Theorem 1

Let $d \in \mathbb{N}$ denote the hidden state dimension. For a given decoding step t , let $q_t \in \mathbb{R}^d$ be the query vector. Let $K_t = [k_1, k_2, \dots, k_t]^\top \in \mathbb{R}^{t \times d}$ and $V_t = [v_1, v_2, \dots, v_t]^\top \in \mathbb{R}^{t \times d}$ be the key and value matrices, respectively, where $k_j, v_j \in \mathbb{R}^d$ for $j = 1, \dots, t$. The unnormalized attention scores, denoted by $S_t \in \mathbb{R}^t$, are given by:

$$S_t = \frac{q_t K_t^\top}{\sqrt{d}}$$

The attention weights $A_t \in \mathbb{R}^t$ are then computed by applying the softmax function to S_t :

$$A_t = \text{softmax}(S_t) = \text{softmax}\left(\frac{q_t K_t^\top}{\sqrt{d}}\right)$$

The output vector $o_t \in \mathbb{R}^d$ at decoding step t is a weighted sum of the value vectors:

$$o_t = \sum_{j=1}^t (A_t)_j v_j$$

Suppose for some $j \in \{1, \dots, t\}$, we replace k_j with k'_j such that $\|k_j - k'_j\| < \varepsilon$, and v_j with v'_j such that $\|v_j - v'_j\| < \delta$. We will analyze the effect of these substitutions on the attention weights and the output o_t .

1. Key Similarity \implies Similar Attention Scores

Let S_t be the vector of unnormalized attention scores with key matrix K_t , and let S'_t be the vector of unnormalized attention scores when k_j is replaced by k'_j in K_t (forming K'_t).

The i -th component of S_t is $(S_t)_i = \frac{q_t k_i^\top}{\sqrt{d}}$. Similarly, the i -th component of S'_t is:

$$(S'_t)_i = \begin{cases} \frac{q_t k_i^\top}{\sqrt{d}}, & i \neq j \\ \frac{q_t (k'_j)^\top}{\sqrt{d}}, & i = j \end{cases}$$

The difference between S_t and S'_t is non-zero only at the j -th position. The magnitude of this difference is:

$$|(S_t)_j - (S'_t)_j| = \left| \frac{q_t k_j^\top}{\sqrt{d}} - \frac{q_t (k'_j)^\top}{\sqrt{d}} \right| = \frac{|q_t (k_j - k'_j)^\top|}{\sqrt{d}}$$

By the Cauchy-Schwarz inequality, $|q_t (k_j - k'_j)^\top| \leq \|q_t\|_2 \|k_j - k'_j\|_2$. Given $\|k_j - k'_j\|_2 < \varepsilon$, we have:

$$|(S_t)_j - (S'_t)_j| < \frac{\|q_t\|_2 \varepsilon}{\sqrt{d}}$$

For $i \neq j$, $(S_t)_i - (S'_t)_i = 0$. Therefore, the ℓ_∞ norm of the difference between S_t and S'_t is:

$$\|S_t - S'_t\|_\infty = \max_i |(S_t)_i - (S'_t)_i| = |(S_t)_j - (S'_t)_j| < \frac{\|q_t\|_2 \varepsilon}{\sqrt{d}}$$

Now, we analyze the effect on the attention weights $A_t = \text{softmax}(S_t)$ and $A'_t = \text{softmax}(S'_t)$. The softmax function $\sigma : \mathbb{R}^t \rightarrow \mathbb{R}^t$ is Lipschitz continuous (Collins et al. 2024;

Virmaux and Scaman 2018). Specifically, for any $x, y \in \mathbb{R}^t$, the following inequality holds:

$$\|\sigma(x) - \sigma(y)\|_1 \leq \|x - y\|_\infty$$

Applying this property to our case, we get:

$$\begin{aligned} \|A_t - A'_t\|_1 &= \|\text{softmax}(S_t) - \text{softmax}(S'_t)\|_1 \\ &\leq \|S_t - S'_t\|_\infty < \frac{\|q_t\|_2 \varepsilon}{\sqrt{d}} \end{aligned}$$

This result demonstrates that a small perturbation in a key vector k_j leads to a linearly bounded change in the ℓ_1 norm of the attention weights, directly proportional to the magnitude of the perturbation ε and the norm of the query vector, and inversely proportional to \sqrt{d} .

2. Value Similarity \implies Small Output Perturbation

Let o_t be the original output and o'_t be the output when only the value vector v_j is replaced by v'_j , while keeping the key matrix K_t (and thus A_t) unchanged. The expressions for o_t and o'_t are:

$$o_t = \sum_{i=1}^t (A_t)_i v_i$$

$$o'_t = \sum_{i \neq j} (A_t)_i v_i + (A_t)_j v'_j$$

The difference between the two outputs is:

$$\|o_t - o'_t\|_2 = \|(A_t)_j v_j - (A_t)_j v'_j\|_2 = |(A_t)_j| \|v_j - v'_j\|_2$$

Since $(A_t)_j$ is a scalar, we have:

$$\|o_t - o'_t\|_2 = |(A_t)_j| \|v_j - v'_j\|_2$$

Given that A_t is a probability distribution, $(A_t)_j \geq 0$ and $\sum_{i=1}^t (A_t)_i = 1$, which implies $(A_t)_j \leq 1$. With $\|v_j - v'_j\|_2 < \delta$, we can write:

$$\|o_t - o'_t\|_2 < (A_t)_j \delta \leq \delta$$

This shows that if only a single value vector is perturbed, the change in the output o_t is directly bounded by the magnitude of the perturbation δ .

More generally, if a set of value vectors indexed by $J \subseteq \{1, \dots, t\}$ are perturbed, i.e., $v_j \rightarrow v'_j$ for all $j \in J$ such that $\|v_j - v'_j\|_2 < \delta$ for all $j \in J$, then by the triangle inequality:

$$\begin{aligned} \|o_t - o'_t\|_2 &= \left\| \sum_{j \in J} (A_t)_j (v_j - v'_j) \right\|_2 \leq \sum_{j \in J} \|(A_t)_j (v_j - v'_j)\|_2 \\ &= \sum_{j \in J} (A_t)_j \|v_j - v'_j\|_2 \\ &\leq \sum_{j \in J} (A_t)_j \delta = \delta \sum_{j \in J} (A_t)_j \end{aligned}$$

Since $\sum_{j \in J} (A_t)_j \leq \sum_{j=1}^t (A_t)_j = 1$, it follows that:

$$\|o_t - o'_t\|_2 < \delta$$

Thus, even with multiple value vector perturbations, the total change in the output is bounded by the maximum perturbation in any individual value vector.

3. Combined Effect on Output

If both k_j and v_j are replaced, the total change in o_t can be decomposed as

$$\|o_t - o_t''\| \leq \|o_t - o_t'\| + \|o_t' - o_t''\|,$$

where o_t' is the output with both $k_j \rightarrow k_j'$ and $v_j \rightarrow v_j'$. The first term is bounded as above. The second term, due to the change in A^t from $k_j \rightarrow k_j'$, is

$$\begin{aligned} \|o_t' - o_t''\| &= \left\| \sum_{i=1}^t (A_i^t - A_i^{t'}) v_i' \right\| \\ &\leq \sum_{i=1}^t |A_i^t - A_i^{t'}| \cdot \|v_i'\| \\ &\leq \|A_t - A_t'\|_1 \cdot \max_i \|v_i'\|. \end{aligned}$$

Assuming $\|v_i'\|$ is bounded (as is typical in practice), this term is $O(\varepsilon)$.

Conclusion.

The above analysis rigorously establishes that, for sufficiently small ε and δ , the perturbations in the attention weights and output are both tightly bounded. Therefore, substituting a key or value vector with a sufficiently close alternative induces only minor changes in the attention output, thereby justifying the validity and effectiveness of KV cache sharing.